

Observation of energetic particle driven axisymmetric mode in the JT-60U tokamak

G. Matsunaga¹, K. Kamiya¹, K. Shinohara¹, N. Miyato², A. Kojima¹,
A. Bierwage² and JT-60 Team

¹Japan Atomic Energy Agency, Naka, Ibaraki 311-0193, Japan

²Japan Atomic Energy Agency, Rokkasho, Aomori 039-3212, Japan

1. Introduction

Toroidally symmetric modes in the frequency range of the geodesic acoustic mode (GAM) are reported in tokamak and helical devices with the neutral beam (NB) or ICRF heated plasmas [1–4]. These modes are thought to be GAMs driven by energetic particles, thus, energetic particle driven GAM (EGAM) [5–7]. Unlike turbulent driven GAM, these modes have observable magnetic fluctuations. In the JT-60U experimental operations with the reversed magnetic shear, magnetic fluctuations with multiple peaks in the GAM frequency range are observed. In this paper, the experimental observations of the axisymmetric modes driven by energetic particles are described.

2. Observation of axisymmetric mode

In the JT-60U reversed shear startup for high- β_N and high boot strap fraction (f_{BS}) experiments, toroidally symmetric (axisymmetric) modes, thus the toroidal mode number is $n = 0$, are observed. Figure 1 shows a typical startup of high- β_N discharge with $I_p/B_t = 0.9\text{MA}/1.58\text{T}$. Namely, the tangential NBs are injected during plasma current I_p ramp up to delay the current penetration. As shown in Fig. 1 (c), three peaks in magnetic fluctuation measured by saddle loops are simultaneously observed around 10 kHz range. Tick line indicates a dependence on electron temperature, thus $\propto \sqrt{T_e}$. During the single injection of tangential NB in the counter (CTR)-direction of I_p , the observed peaks are followed $\sqrt{T_e}$. The electron temperature at the center T_{e0} gradually increased and the line averaged electron densities are almost constant. After the tangential NB in the co-direction of I_p , the modes are weakened or disappeared. Note that one of the modes survived just before the H mode transition.

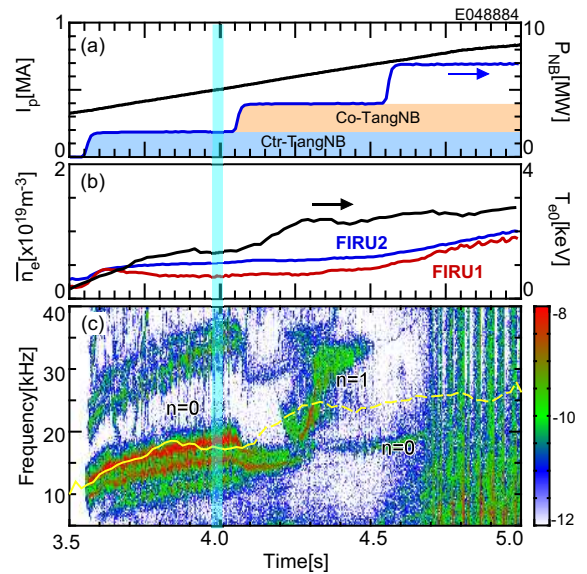


Fig 1: Time evolutions of (a) Plasma current and NB injection power, (b) line-averaged electron densities (red: core, blue: edge) and electron temperature at center and (c) spectrogram of magnetic fluctuation with GAM frequency.

Figure 2 shows the power spectra of the observed electron densities and magnetic fluctuations. In JT-60U, line integrated electron densities at edge and core region are measured by interferometers with different sight lines (FIR1 and 2) as shown in Fig. 2(c). Mirnov signal in Fig. 2(b) clearly shows three peaks ($f = f_1, f_2$ and f_3) around 10 kHz range at $t = 4.0$ s. The peak at the lowest frequency ($f = f_1$) is detected at the edge region by FIR1 indicating that this peak is localized or has amplitude at $\rho \geq 0.9$. On the other hand, higher frequency peaks

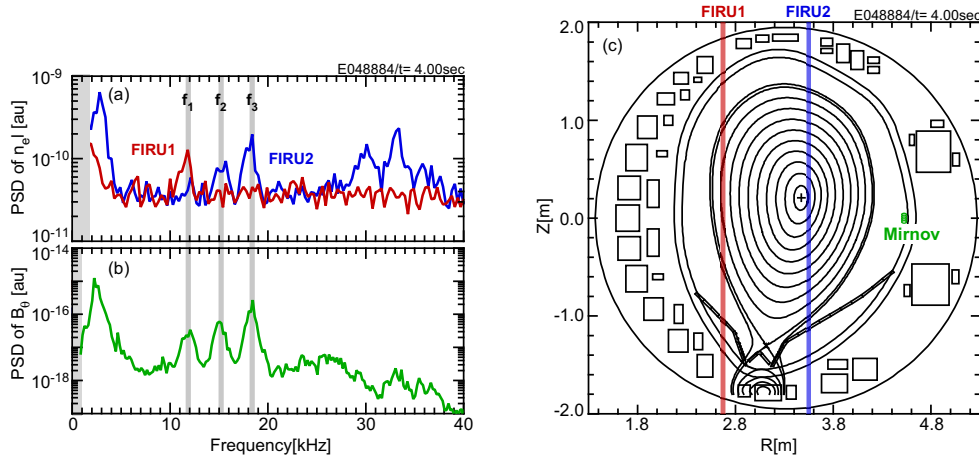


Fig 2: Power spectra of observed peaks: (a) electron density and (b) magnetic fluctuations. (c) Plasma configuration with sight lines of FIR for electron density measurement and Mirnov location.

($f = f_2$ and f_3) are only observed by FIR2 that through the plasma core region. Note that the much lower frequency peak around 3 kHz is $m/n = 6/1$ mode structure, where n and m are the toroidal and poloidal mode number, respectively. Since the edge safety factor q_{95} is just below 6.0, the mode is thought to be an island at the edge region.

3. Mode structures

In JT-60U, mode structures of magnetic fluctuation can be identified by toroidally distributed 8 saddle loops and poloidally distributed 16 Mirnov probes. Figure 3 shows the toroidal (upper panels) and poloidal (lower panels) phase differences for the observed peaks. Every peaks have clear $n = 0$ axisymmetric toroidal mode structures and $m = 2$ poloidal ones. The peaks at $f = f_1$ and f_2 are propagating in the ion and electron diamagnetic poloidal directions. Interestingly, the poloidal mode structure sometimes behaves like standing wave, for example the peak at $f = f_3$. Namely, the standing wave means that $m = 2$ components in both ion ($m > 0$) and electron ($m < 0$) diamagnetic directions are coexist. The standing wave nodes are located around the inboard and outboard on the mid-plane, and the top and bottom of plasmas. Whether the peaks are propagating or standing is changing with time. The $m = \pm 2$ poloidal structure in magnetic fluctuation for GAM, that is due to the $m = 2$ parallel return current, is theoretically predicted [8, 9]. Primarily, the GAM is predicted to have only potential and pressure perturbations. However, the $m = 2$ magnetic GAM structures are derived from the higher order in inverse aspect ratio ε .

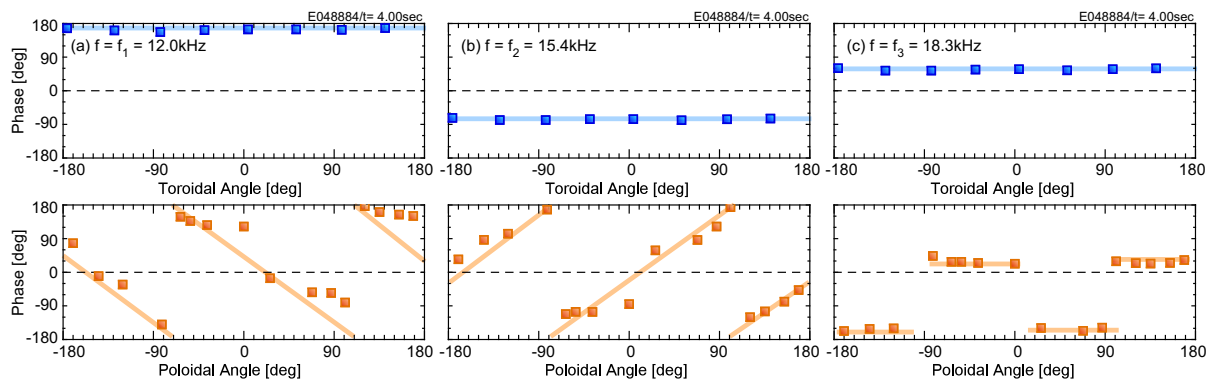


Fig 3: Toroidal (upper) and poloidal (lower) mode structures of simultaneously observed peaks: (a) $f = 12.0$ kHz, (b) $f = 15.4$ kHz and (c) $f = 18.3$ kHz.

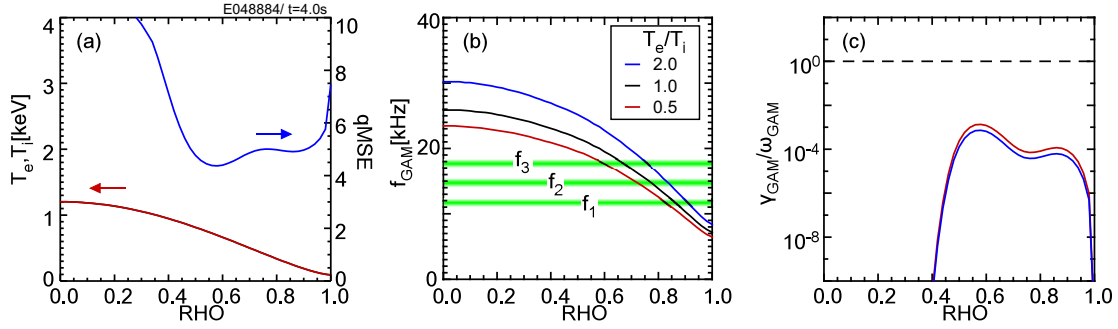


Fig 4: Profiles of (a) T_e and q , (b) GAM frequencies with different T_e/T_i ($= 0.5, 1.0$ and 2.0) and (c) GAM damping rates (red: Ref. [10], blue: Ref. [11]).

The $m = \pm 2$ magnetic GAM structures are directly observed for the first time in the tokamak devices.

In Refs of [10, 11], the GAM eigenvalue $\omega_0 = \omega_G + i\gamma_G$ is provided. The real frequency ω_G includes the q dependence and imaginary one takes into account the Landau damping effect. Figure 4 shows the profiles of the GAM frequencies and damping rates estimated by using the formulas in these Refs and the experimentally obtained T_e and q profiles. The GAM is characterized by the ion temperature T_i , however, T_i profile was not measured in this phase. As shown in Fig. 4(b), the GAM frequencies are estimated by $T_e/T_i = 0.5, 1.0$ and 2.0 . Since a ion-electron equipartition time is $\tau_{\text{eq}} \sim 0.3$ s, the ion temperature is thought to be comparable to T_e , thus, $T_e/T_i \simeq 1.0$. The observed three peaks are indicated as horizontal lines. In the region of $\rho \geq 0.45$, the GAM damping rates γ_G/ω_G are larger, thus, 0.01-0.1%, due to small q -values.

4. Energetic particles on Co and CTR NB injections

The GAM peaks are observed after tangential NB injections with the beam energy of 85 keV. In particular, the mode amplitudes in the CTR-injection case are much larger than in the CO-injection as shown in Fig. 5. To pick up $n = 0$ component in the magnetic fluctuations, the averaged signal among 8 saddle loops distributed almost regular intervals toroidally is used, thus $B_r^{n=0} \simeq B_r^{\text{avg}} = \sum B_r^i / N$; this average operation can cancel out $n \neq 0$ components.

To find out this difference of the GAM drive, orbits of energetic particles injected from the CO- and CTR-NBs are calculated by F3D-OFMC [12]. Figure 6 shows energetic particle pressure profiles and distributions in velocity space in CO- and CTR-cases. These are statistical results on the flux surface, not across the mid-plane, as steady state with the slowing down time of about 0.4 s. In the core region, pressure in the CO-injection is about 50% larger than in the CTR-injection. The inversions ($\partial f / \partial E > 0$) in velocity distributions can not be seen at the steady state, although these exist until ~ 0.1 s after NB injection in both injection cases. Both pressures are almost similar in the region of $\rho \geq 0.4$. Differences between the CO- and CTR-injection can be seen in Fig. 6(b) and (c) due to trapped particles around

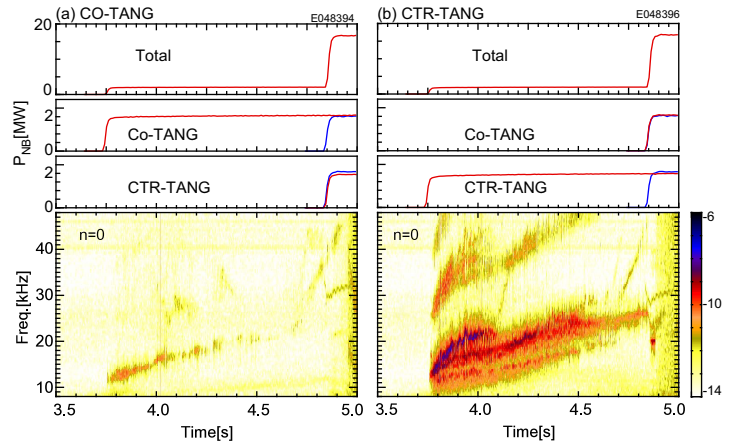


Fig 5: Comparison of GAM behavior with (a) CO- and (b) CTR-NB injections. Magnetic spectrograms are analyzed as $n = 0$ component.

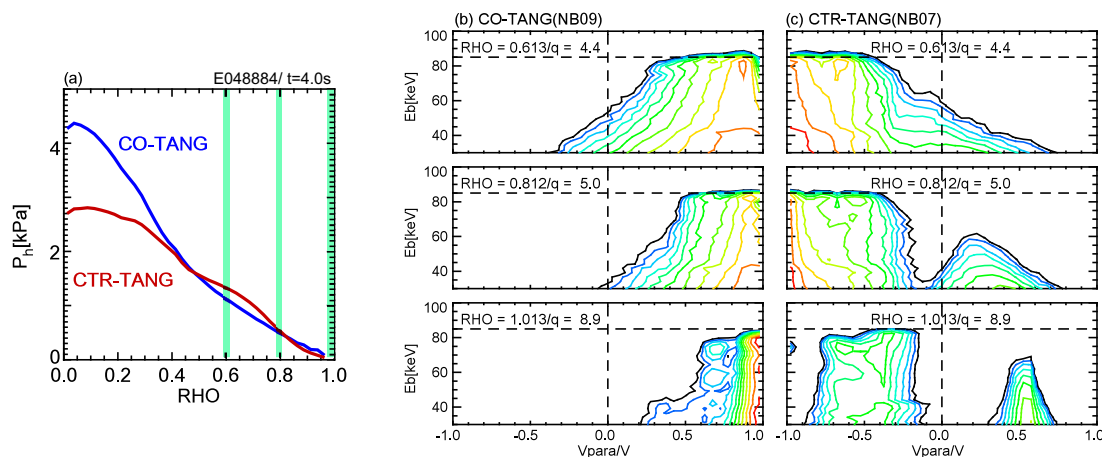


Fig 6: (a) Energetic particle pressure profiles and distributions in velocity space: (b) CO- and (c) CTR-NB injections with different radial location ($\rho \simeq 0.6, 0.8$ and 1.0).

$v_{\parallel}/v \sim 0.5$ only in the CTR-injection. At the moment, it is not clear how the GAMs are excited with these velocity distributions. The difference between the CO- and CTR-injections implies that the trapped particles may play an important role in the GAM excitation.

5. Summary

In the JT-60U experimental operations with the reversed magnetic shear, the $n = 0$ magnetic fluctuations with multiple peaks in the GAM frequency range are observed. From the observation of (i) the observed frequencies depending on the electron temperature, (ii) the toroidally symmetric mode structures, (iii) the poloidal magnetic structure being the same as the theoretical prediction, (iv) clear correlation between mode appearance and NB injection timing, the observed modes are thought to be the GAMs driven by energetic particles. In particular, the poloidal magnetic structures with $m = 2$ propagating in the both ion and electron diamagnetic direction and being standing wave are directly observed in tokamak devices for the first time. Moreover, the mode amplitude in the CTR-injection is much larger than in the CO-injection. Although this difference of the CO- and CTR-injections is still unclear, velocity distribution at $\rho \geq 0.6$ are quite different due to trapped particles.

This work was supported in part by a Grant-in-Aid for Young Scientists (B) from the Ministry of Education, Culture, Sports, Science, and Technology of Japan, No. 23760818.

References

- [1] H. L. Berk, et al., *Nuclear Fusion* **46**, S888 (2006).
- [2] R. Nazikian, et al., *Phys. Rev. Lett.* **101**, 185001 (2008).
- [3] K. Toi, et al., *Phys. Rev. Lett.* **105**, 145003 (2010).
- [4] T. Ido, et al., *Nuclear Fusion* **51**, 073046 (2011).
- [5] G. Y. Fu, *Phys. Rev. Lett.* **101**, 185002 (2008).
- [6] H. L. Berk and T. Zhou, *Nuclear Fusion* **50**, 035007 (2010).
- [7] Z. Qiu, et al., *Plasma Phys. Control. Fusion* **52**, 095003 (2010).
- [8] D. Zhou, *Phys. of Plasmas* **14**, 104502 (2007).
- [9] C. Wahlberg, *Plasma Phys. Control. Fusion* **51**, 085006 (2009).
- [10] H. Sugama and T. H. Watanabe, *J. Plasmas Phys.* **72**, 825 (2006).
- [11] M. Sasaki et al., *Plasma Fusion Res.* **3**, 009 (2008).
- [12] K. Shinohara et al., *Nuclear Fusion* **47**, 997 (2007).